

Components explain, but do eddy fluxes constrain? Carbon budget of a nitrogen-fertilized boreal Scots pine forest

John D. Marshall^{1,2} , Lasse Tarvainen^{1,3} , Peng Zhao¹ , Hyungwoo Lim^{1,4} , Göran Wallin^{3,5} ,
Torgny Näsholm¹ , Tomas Lundmark¹ , Sune Linder⁶  and Matthias Peichl¹ 

¹Department of Forest Ecology and Management, Swedish University of Agricultural Sciences (SLU), Umeå SE-901 83, Sweden; ²Leibniz-Zentrum für Agrarlandschaftsforschung, Isotopen-Biogeochemie und Gasflüsse, Müncheberg 15374, Germany; ³Department of Biological and Environmental Sciences, University of Gothenburg, Gothenburg SE-405 30, Sweden; ⁴Institute of Ecology and Earth Sciences, University of Tartu, Juhan Liivi 2, Tartu 50409, Estonia; ⁵Environmental Change Institute, School of Geography and the Environment, University of Oxford, South Parks Road, Oxford, OX1 3QY, UK; ⁶Southern Swedish Forest Research Centre, SLU, PO Box 190, Lomma SE-234 22, Sweden

Summary

Author for correspondence:
John D. Marshall
Email: john.marshall@slu.se

Received: 5 November 2022
Accepted: 22 March 2023

New Phytologist (2023) 239: 2166–2179
doi: 10.1111/nph.18939

Key words: canopy photosynthesis, carbon flux partitioning, carbon sequestration, carbon-use efficiency, eddy covariance, nitrogen fertilization.

- Nitrogen (N) fertilization increases biomass and soil organic carbon (SOC) accumulation in boreal pine forests, but the underlying mechanisms remain uncertain. At two Scots pine sites, one undergoing annual N fertilization and the other a reference, we sought to explain these responses.
- We measured component fluxes, including biomass production, SOC accumulation, and respiration, and summed them into carbon budgets. We compared the resulting summations to ecosystem fluxes measured by eddy covariance.
- N fertilization increased most component fluxes ($P < 0.05$), especially SOC accumulation (20×). Only fine-root, mycorrhiza, and exudate production decreased, by 237 (SD = 28) g C m⁻² yr⁻¹. Stemwood production increases were ascribed to this partitioning shift, gross primary production (GPP), and carbon-use efficiency, in that order. The methods agreed in their estimates of GPP in both stands ($P > 0.05$), but the components detected an increase in net ecosystem production (NEP) (190 (54) g C m⁻² yr⁻¹; $P < 0.01$) that eddy covariance did not (19 (62) g C m⁻² yr⁻¹; ns).
- The pairing of plots, the simplicity of the sites, and the strength of response provide a compelling description of N effects on the C budget. However, the disagreement between methods calls for further paired tests of N fertilization effects in simple forest ecosystems.

Introduction

Ecosystem carbon budgets represent the cumulative CO₂ exchange between ecosystems and the atmosphere, often quantified using the eddy covariance (EC) technique (Baldocchi, 2008; Monson & Baldocchi, 2014). These measurements describe the net exchange between the whole ecosystem and the atmosphere, integrated over a footprint upwind of the measurement point. Alternatively, carbon budgets can be derived by summing the individual C cycle components, including biomass production, soil carbon changes, and respiratory fluxes using inventory and chamber techniques (Peichl *et al.*, 2010; Lim *et al.*, 2015; Campioli *et al.*, 2016; Eastman *et al.*, 2021). Such changes can be difficult to measure, especially on tissues with rapid turnover such as leaves, roots, and mycorrhizal hyphae. The changes can also be difficult to detect against large background variation, especially in natural forest ecosystems.

Previous studies have compared component fluxes to eddy covariance in boreal forests (e.g. Zha *et al.*, 2007; Goulden *et al.*, 2011). We focus here on the broad-ranging summary of Campioli *et al.* (2016), from which we have drawn several conclusions that are

particularly relevant here. First, they noted that eddy covariance uses a standardized set of protocols, but that the component flux method, which they termed ‘Biometric’, is in fact an unstandardized mixture of different methods and approaches. Second, they noted that boreal forests tended to be especially problematic in method comparisons, perhaps due to low fluxes. Third, they described the range of methods used for measuring respiration fluxes; the nonsteady-state through-flow chambers (NSF) were noted for higher respiration fluxes than from EC methods. Fourth, they noted that daytime extrapolation of ecosystem respiration should be reduced to account for the reduction in leaf respiration during the day (e.g. Wehr *et al.*, 2016). Finally, they noted that any disagreement between the methods could come from either side or both. Here, we compare and synthesize data from biometric and EC methods to develop a detailed component budget for a system that is extremely simple: a boreal monoculture of mature Scots pine (*Pinus sylvestris* L.) with a sparse understory growing in deep sandy deposits that began with low soil organic matter accumulations. One stand had undergone high rates of annual fertilization for 15 yr, the other was unfertilized but otherwise similar at the beginning of the study.

Nitrogen (N) fertilization can change growth and carbon budgets by a limited set of mechanisms. One possibility is that canopy photosynthesis would be increased as a consequence of increased light interception due to increased leaf area index (LAI) and/or increased photosynthetic rates per leaf area. Another alternative is that carbon partitioning may be altered. Here, we discuss this question in terms of total belowground carbon flux (TBCF), the proportion of gross primary production (GPP) that is transported belowground as sugars in the phloem of the plants in the ecosystem (Giardina & Ryan, 2002; Litton *et al.*, 2007; Eastman *et al.*, 2021). TBCF is measured by difference after measuring all other major components of the carbon budget. Critical in this analysis is the accumulation of soil organic matter, which is rapid in fertilized forests (e.g. Olsson *et al.*, 2005; Maaroufi *et al.*, 2015; Forsmark *et al.*, 2020; Marshall *et al.*, 2021). An N-induced increase in aboveground partitioning has been inferred previously at our site (Lim *et al.*, 2015) and in other boreal Scots pine forests (Linder & Axelsson, 1982; Axelsson & Axelsson, 1986), but we note that these estimates relied on models based on untested assumptions.

A last possible cause of the growth increase is an increase in carbon-use efficiency (CUE), which describes the proportion of photosynthate fixed into biomass. We define it here as net primary production (NPP) divided by GPP. This definition of CUE is derived from the concept of 'growth yield' (e.g. Vertregt & Penning de Vries, 1987), but we pick it up with Waring's claim (Waring *et al.*, 1998) that the efficiency is constant. This claim has provoked several challenges (Medlyn, 1998; Mäkelä & Valentine, 2001; Vicca *et al.*, 2012; Collalti & Prentice, 2019). Even after a recent response by Landsberg *et al.* (2020), the question remains unresolved. Part of the difficulty is the different definitions of CUE that have been applied (Capioli *et al.*, 2015; Manzoni *et al.*, 2018). We focus on aboveground CUE, which includes only autotrophic processes, sharply constraining the possible range of values.

We had two objectives: (1) to use the ecophysiological information in the compartmental fluxes to identify the mechanisms underlying the nitrogen-induced growth increase in the overstorey pine trees and (2) to compare the bottom-up compartmental flux method to the top-down eddy flux method of measuring ecosystem fluxes on a heavily and continuously nitrogen-fertilized plot and on a nearby unfertilized reference plot. The treatment effect on biomass production and soil organic matter accumulation was exceptionally strong due to a 15-yr annual fertilization regime with nitrogen. Given the stand uniformity, the low baseline, and the extreme treatment, the signal-to-noise ratio was expected to be as high as in any forest ecosystem yet studied.

Materials and Methods

This study combines rigorous measurements by eddy covariance with measurements of chamber fluxes and pool accumulations. Some of these components are taken from previous publications, but many (e.g. litterfall and biomass production) are extended in time beyond previous reports or reported for the first time (e.g. shoot and stem respiration). Many of the component fluxes were

measured intensively in 2012–2014, the eddy covariance data were measured in 2015–2019, and some of the component fluxes were measured throughout (2012–2019). We provide detailed descriptions of the measurements and data sources in Table 1. The integration to the whole stand has previously been reported for eddy covariance (Zhao *et al.*, 2022), but it has never been attempted from the components.

Study site

The research was conducted at Rosinedalsheden, a paired set of field experimental sites established in 2005 (Fig. 1). The canopy is comprised of even-aged Scots pine (*Pinus sylvestris* L.) trees *c.* 100 yr of age. The site is located *c.* 5 km southeast of Vindeln, Sweden (64°10'N, 19°45'E, 145 m above sea level (asl)) on a flat, sandy deposit formed where the Vindeln River once entered the Baltic Sea. Isostatic lift has caused the land to rise since glacial times. The stand was naturally regenerated following a fire and has been mechanically thinned twice, most recently in 1993. The 33-yr mean annual temperature and precipitation (1981–2013), measured at the Svartberget research station, 8 km from the study site, were 1.8°C and 614 mm, respectively (Laudon *et al.*, 2013). On average, snow cover lasts from late October to early May. The soil is a weakly developed podzol with an organic mor layer ranging in thickness from 2 to 5 cm (Hasselquist *et al.*, 2012). The depth to the water table is at least 10 m (H. Laudon, pers. comm.).

The paired sites were chosen to have similar characteristics and were used to compare flux components in the presence and absence of N addition. One of the 13-ha plots (F) has been fertilized annually since 2006. The fertilization rate began at 100 kg ha⁻¹ yr⁻¹, from 2006 to 2011. From 2012 onward, the rate was reduced because we detected nitrate (*c.* 3 mg NO₃⁻N l⁻¹) in suction lysimeters at 60 cm depth. After 2012, these reduced fertilization rates varied somewhat due to a mistake by the field crew. They were 50 kg N ha⁻¹ yr⁻¹ in 2012–2014 and 2016 and were 64 kg N ha⁻¹ yr⁻¹ in 2015 and 2017 and thereafter. Thus, the cumulative nitrogen addition by the year 2020 was 1120 kg N m⁻². Of these additions, 90% remained in the understory, litter layer, and surface 20 cm of mineral soil in 2020 (H. Lim, pers. obs.). The fertilizer was pelletized ammonium nitrate Skog-Can fertilizer (Yara, Sweden), containing NH₄⁺ (13.5%), NO₃⁻ (13.5%), Ca (5%), Mg (2.4%), and B (0.2%; Lim *et al.*, 2015). The unfertilized site was left as a 'control', but because neither the control nor the fertilization was replicated, we refer to the unfertilized plot as the 'Reference' (R) stand from here forward.

As the experimental design did not provide true replication of the nitrogen fertilization treatments, we treat the experiment as a case study and account for pretreatment differences in stand and site characteristics insofar as possible. A previous study concluded that the pretreatment differences had little influence on production parameters in the C budget (Lim *et al.*, 2015). Ecosystem fluxes were similar between the two plots in 2006, including several months before the fertilization and several afterward (Zhao *et al.*, 2022), so we believe the comparison is valid. Stand characteristics are summarized for 2013 in Table 2.

Table 1 Summary of component and eddy covariance measurements, including citations for methods and data previously published, in a nitrogen-fertilized Scots pine experiment.

Method	No. in Table 3	Component	Year(s) ^a	Measurement seasons ^b	Technique	Climate control ^c	Individual sample sizes	Replication per plot	Measurement frequency	References
<i>Gas exchange with chambers</i>										
	1	Respiration tree foliage	2013–2016	April–October	Steady-state through-flow chambers; Air turnover: twice per minute	T track ambient	5.5 cm shoot previous year shoot, volume 0.5 l, 2 canopy layers	4	30 min	Tarvainen <i>et al.</i> (2016)
	2	Respiration stems and branches	2013–2016	April–November	Steady-state through-flow chambers; Air turnover: once-twice per minute	None, but shielded	109–126 cm ² stem, 4 stem heights	2–5	30 min	Tarvainen <i>et al.</i> (2018)
	11, 14	Understory photosynthesis and soil respiration	2012–2014	May/June–October/November	Nonsteady-state through-flow chambers; Air turnover: once per 30 min	T track ambient	Soil area 20 m ² , volume 18 m ³	2	30 min	Marshall <i>et al.</i> (2021)
<i>Mass production and allometry</i>										
	3, 4	Litterfall and cone litter	2012–2016	Whole year	Samples from litter traps separated into foliage, cones, bark, branches, and miscellaneous	na	0.25 m ²	11	Twice per year (spring and autumn)	Lim <i>et al.</i> (2015)
	5, 6, 12	Stem, branch and coarse root production	2006, 2011, 2018	Whole year	Site-specific allometric equations developed from harvested trees	na	Aboveground part of trees of different sizes (2006, 2011, 2018); belowground coarse roots (≥ 2 cm, 2011)	15, 6, 6 trees from 2006 ^d , 2011, 2018	Before, and 6- and 13-yr after treatment	Lim <i>et al.</i> (2015)
	13	Soil organic carbon production	2012–2018	Whole year	Biomass estimates from diameter at breast-height, crown length, and wood density measurements using the site-specific allometric equations	na	Plot area 1000 m ²	3	Once per year, outside growing season	Lim <i>et al.</i> (2015)
<i>Eddy covariance</i>										
		Net ecosystem production, gross primary production, ecosystem respiration	2015–2019	Whole year	Closed-path analyzers, corrected for decoupling	na	78.5 cm ² samples of vegetation, organic layer, 0–5, and 5–10 cm mineral soil	13 per plot	Once	Marshall <i>et al.</i> (2021)
						na	94% of time, 80% of source area within plot	None	20 Hz	Zhao <i>et al.</i> (2022)

The numeral in the second column describes the line in Table 3 for which the measurement was used.
^aYears mean the period of measurements and/or modeling.
^bThe valid season for measurement and/or modeling.
^cT, temperature; na, not applicable.
^dReplicates from plots of harvested trees before treatment start were lumped together.

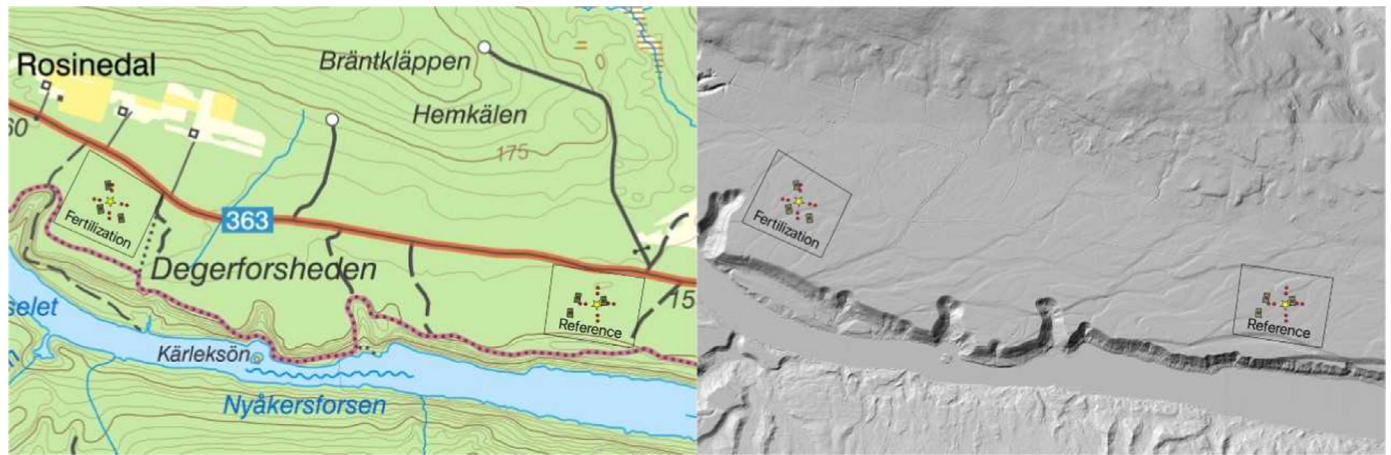


Fig. 1 Map and digital elevation model of the Rosinedal study area, near Vindeln, Sweden, showing the location of the Fertilized and Reference plot. Symbols: eddy flux tower, litter trap, mensuration plot.

Table 2 Scots pine stand characteristics in 2013, the middle year of the CO₂ efflux measurements presented here.

Characteristic	Reference plot	Fertilized plot	Source
Density (trees ha ⁻¹)	1010 (125)	857 (83)	Lim <i>et al.</i> (2015)
Diameter (cm)	18.6 (0.1)	19.1 (0.5)	Lim <i>et al.</i> (2015)
Height (m)	17.5 (<0.1)	16.6 (0.2)	Lim <i>et al.</i> (2015)
Stem volume (m ³ ha ⁻¹)	237 (28)	201 (14)	Lim <i>et al.</i> (2015)
Tree leaf area index (LAI)	2.6	3.4	Tian <i>et al.</i> (2021)
LAI of ground vegetation	1.0	0.5	Tian <i>et al.</i> (2021)

The SDs are presented in parentheses.

Chamber measurements of soil, stem and leaf CO₂ fluxes

Understory fluxes and soil respiration were measured as net CO₂ exchange using four large chambers, two each in the fertilized and reference stands. The chambers are described in detail in Marshall *et al.* (2021). Briefly, the chambers contained ducted fans at the inlet and the outlet; the valves opened and the fans flushed the chamber air every 30 min. After flushing, the valves closed and the increase in chamber CO₂ concentrations was monitored. The chambers were cooled by a thermostatted heat exchanger. For measurement frequency and periods, see Table 1.

The chambers were placed to bracket differences in vegetation types. The ground vegetation on the plots was dominated by bilberry, cowberry, heather (*Vaccinium myrtillus* L., *Vaccinium vitis-idaea* L., *Calluna vulgaris* (L.) Hull), mosses, and lichens, but the chamber area was covered by a Scots pine canopy. The most obvious source of variation across the plots was in bilberry cover. Therefore, throughout the experiment, two of the chambers were always placed in areas with > 25% bilberry cover and two others always had < 10% bilberry cover. The locations of the large chambers were thus not random, but chosen to sample the range of vegetation composition.

A nonlinear model was fitted to the CO₂ flux data using JMP PRO 11.0.0 (SAS Institute, Cary, NC, USA). We simultaneously fitted parameters to a nonlinear function, including a Q_{10} temperature-response and a Michaelis–Menten light-response curve modified by a soil moisture response term, as follows:

$$\text{Net CO}_2 \text{ efflux} = R_{0m} \times Q_{10m}^{(T/10)} + \text{GPP}_{\text{maxm}} \times (\text{PAR}/(\text{PAR} + K_m)) - b(\theta - \theta_{fc}), \quad \text{Eqn 1}$$

where T is the measured air temperature, PAR is the photosynthetically active radiation measured above the canopy, θ is the volumetric soil moisture content at 15 cm depth, θ_{fc} is the volumetric soil moisture content at field capacity, b is an empirical parameter describing the sensitivity of the efflux to soil moisture, and R_{0m} is the monthly basal efflux rate (at 0°C). We used the fitted model to predict the dark CO₂ flux into the chambers throughout each day and throughout the year by setting PAR to zero and rerunning the models. This was done to remove understory GPP from the measured net efflux. The second term in the model was then used, under ambient conditions, to estimate GPP of the understory vegetation.

Respiration rates of shoot segments were fitted using continuous cuvette data gathered in the year 2013 on shoots produced in 2012, from two canopy layers (sunlit upper canopy and shaded lower canopy). For an overview of the sample design, see Table 1, and for measurement details, see Tarvainen *et al.* (2016). All data were filtered to eliminate photosynthesis using a PPFD threshold of 2 $\mu\text{mol m}^{-2} \text{s}^{-1}$ and placed in 2.5°C bins and averaged over each individual shoot for each month. Thereafter, the data were fitted with an exponential function to obtain the base dark respiration rate (R_{d0}) and its temperature dependency (Q_{10}). Data from months and shoots that yielded low R^2 values were not used to calculate Q_{10} . Finally, the remaining shoot-specific monthly values were averaged for each layer and used as model parameters assuming a two-layer canopy based on needle mass distribution within the canopies (Lim *et al.*, 2015). Respiration rates for 2013–2016 were estimated using the parameters from 2013 and temperature data from each year using the Maestra

model (Wang & Jarvis, 1990; Duursma & Medlyn, 2012). The cuvette measurements were made in April–October, and model parameters R_{d0} and Q_{10} were updated on the 15th of each month during this period, with the October parameters used to represent the winter months. Previous measurements compared needle-age cohorts and found no effect, so we did not account for one. See Supporting Information Methods S1 for a discussion of this assumption. Needle biomass was allowed to vary based on LAI corrected for seasonal changes using estimates of leaf turnover through the growing season. The leaf respiration data are corrected downward in the daytime to account for the Kok Effect (Wehr *et al.*, 2016). As detailed in Stangl *et al.* (2022), we predicted respiration based on the nighttime respiration–temperature relationship but then decreased the value downward by 40% (Way & Yamori, 2014) whenever the PPFD was $> 2 \mu\text{mol m}^{-2} \text{s}^{-1}$.

Stem respiration rate was calculated from continuous observations. The methods were mostly similar to earlier reports from this site (Tarvainen *et al.*, 2018). In brief, the stem efflux was measured for 4 yr on two and five trees on the reference and fertilized plots, respectively. The measurements were made at 1.5 m height and were mostly continuous except during rare technical breakdowns. Vertical variation (four heights) in stem respiration and branch respiration were determined in 2013 and extrapolated to describe the other years assuming a constant ratio between them and the measurements at 1.5 m in all years. Stem surface area and branch area were estimated as in Tarvainen *et al.* (2018). The November values were assumed representative of the December–March period when no measurements were made.

We estimated aboveground carbon-use efficiency (ACUE) by first calculating aboveground GPP (AGPP). This was done by adding the sum of aboveground respiration to the sum of aboveground NPP (ANPP; Table 3). By then dividing ANPP by AGPP, we estimated ACUE. A similar analysis was performed for stem and branch growth alone using only the data from the stems and branches. Belowground CUE is described below.

Standing stock, volume increment, and litterfall

Estimates of standing stock and annual increments were based on regular measurements of breast height diameter, height, and length of live crown used in site-specific allometric equations modified using additional harvested sample trees (12 trees from 2018) from those presented by Lim *et al.* (2015; 15 trees harvested in 2006 and 12 trees in 2012). As the measurements were made in different seasons, the annual production required *post hoc* adjustment. This was done using ring widths measured from increment cores. See Methods S2 for a discussion of mortality effects on these estimates.

Eleven litter traps were installed around the towers in each stand in June 2006 (Fig. 1; Table 1). The collected litterfall was sorted into foliage, cones, bark, dead branches, and miscellaneous. The carbon concentration of litter was measured on a Flash EA 2000 (Thermo Fisher Scientific, Waltham, MA, USA) elemental analyzer.

Assessment of soil carbon pools and accumulation rates

Soil samples were collected in September 2020, after 15 yr of N addition totaling 112 g N m^{-2} . The C accumulation per N addition was 20.8 g g^{-1} , which is similar to the $22.3 \text{ g C g N}^{-1}$ of Forsmark *et al.* (2020) on a similar site as well as the 19 g C g N^{-1} in a global meta-analysis (Janssens *et al.*, 2010). This similarity in stoichiometry leads us consider that the C accumulation had not saturated during this period, allowing us to calculate the C accumulation from the yearly N additions. We assumed the baseline C accumulation rate on the Reference plot was $5 \text{ (SD = 1.4) g C m}^{-2} \text{ yr}^{-1}$ based on Peltoniemi *et al.* (2004).

Total belowground carbon flux (TBCF, $\text{g C m}^{-2} \text{ yr}^{-1}$) was estimated by difference as:

$$\text{TBCF} = R_s + \Delta\text{SOC} + \Delta\text{CR} - \text{LF}, \quad \text{Eqn 2}$$

where R_s is cumulative annual soil respiration, ΔSOC is the annual increase in soil organic matter, ΔCR is the annual increase in coarse root biomass, and LF is annual aboveground litterfall (Raich & Nadelhoffer, 1989; Giardina & Ryan, 2002; Ryan *et al.*, 2004; Litton *et al.*, 2007; Halbritter *et al.*, 2020). The ΔCR term was estimated from allometric equations generated at the site and applied to mean tree diameter data from three mensuration subplots (rectangular, 1000 m^2) on each plot (Lim *et al.*, 2015). Lysimeter data (not presented) showed that dissolved organic carbon concentrations were so low that the leaching flux could be neglected in the TBCF calculation.

We estimated belowground CUE (BCUE) as:

$$\text{BCUE} = 1 - (R_a + R_r) / \text{TBCF}, \quad \text{Eqn 3}$$

where R_a is autotrophic respiration from the forest floor. This parameter from the Pumpanen *et al.* (2015) model underestimates true R_a because it does not account for the maintenance respiration of fine roots, which continues during the wintertime (Marshall *et al.*, 2021). We have therefore added in R_r as an estimate of root respiration. R_r was estimated using the Widén & Majdi (2011) temperature–response curve for Scots pine fine roots, fine-root biomass from Lim *et al.* (2015), and the measured daily soil temperatures, as measured on-site at 15 cm depth, for the whole year.

Assessment of foliar nitrogen concentration

To describe the approach to steady state of foliar nutrient concentrations, 1-year-old needles were annually sampled from the upper third of the crowns. Intended as a diagnostic measure rather than to represent the whole crown, the samples were collected in late autumn or winter when starch reserves were depleted and would not dilute the N. After drying at 85°C for 48 h, the samples were ground in a ball mill (MM200; Retsch GmbH, Haan, Germany) and analyzed for C and N using an elemental analyzer (Flash EA 2000; Thermo Fisher Scientific) at the SLU analytical laboratory.

NEP measurements using eddy covariance technique

Eddy covariance was measured above the canopy in 2006, at the beginning of the fertilization, as described by Zhao *et al.* (2022). From July 2014 to present, the EC system above the forest canopy consisted of a Gill R3-100 (Gill Instruments Ltd, Hampshire, UK) sonic anemometer for detecting wind components and sonic temperature and a LI-7200 (Li-Cor Environmental, Lincoln, NE, USA) gas analyzer for detecting H₂O and CO₂ mixing ratios at 20 Hz frequency (Jocher *et al.*, 2017; Zhao *et al.*, 2022). The EC measurement heights were raised to adjust for the continuous increase in tree height. The step-wise rise of the measurement height ensured that the main flux source area (i.e. fetch distance) remained constant and limited to the area of interest.

A second EC system was installed on both plots below the forest canopy at 2.5 m height. These systems (CPEC 200; Campbell Scientific Inc., Logan, UT, USA) consisted of a closed-path infrared gas analyzer (IRGA, EC155; Campbell Scientific) and a three-dimensional ultrasonic anemometer (CSAT3A; Campbell Scientific Inc.). Data from the below- and above-canopy EC systems were used to determine periods of decoupling of below- and above-canopy air masses. The EC raw data were processed using the EDDYPRO[®] software (v.7.0.6; Li-Cor Biosciences) to obtain the 30-min average turbulent fluxes of CO₂. We applied the same corrections, spike filtering, and gap-filling protocols as described in Zhao *et al.* (2022). GPP and ecosystem respiration (R_{eco}) were estimated using the nighttime-based flux partitioning method (Reichstein *et al.*, 2005).

Error propagation and comparison

Errors were propagated using the standard deviations based on annual sums. Standard deviations were chosen to eliminate the effects of differences in sample size, and annual sums were chosen to integrate over seasonal variation. The terms were combined using standard Gaussian approaches, as described in Methods S3.

Results

The Fertilized plot responded gradually to the annual N additions, arriving at a new steady state after *c.* 5 yr. The new steady state was reflected in several of the annual measurements, including litterfall, foliar N concentration, stemwood production, and net ecosystem production (NEP) (Fig. 2). It included year-to-year variation, but no obvious trend and nearly constant differences between the treatments. We focus our comparisons here on the years after the new steady state had been reached, beginning in 2012 and continuing until 2019.

Aboveground component fluxes

Production of stem and branch wood increased dramatically in the first 6 yr of fertilization, more than doubling by 2011. The differences then stabilized at 63 ± 14 (SD) g C m⁻² yr⁻¹ (Fig. 2; Table 3). The increase in wood volume was even greater than the increase in the mass of C because the density of the wood fell

Table 3 Summary of component fluxes (g C m⁻² yr⁻¹) and aboveground carbon-use efficiency (unitless) for the Reference and Fertilized Scots pine plots.

Component fluxes	Reference g C m ⁻² yr ⁻¹	Fertilized
<i>Aboveground</i>		
(1) Respiration tree foliage	210 (8)	281 (9)***
(2) Respiration stems and branches	93 (10)	111 (16) ^{ns}
(3) Leaf litterfall	87 (14)	151 (11)**
(4) Female cone production	5 (0.1)	9 (0.1)***
(5) Stem biomass production	106 (9)	169 (10)**
(6) Branch production	10 (2)	28 (3)**
(7) Tree ANPP [3 + 4 + 5 + 6]	208 (17)	357 (16)***
(8) Tree aboveground respiration [1 + 2]	303 (13)	392 (18)**
(9) Stem and branch CUE [5/(5 + 2)]	0.53 (0.02)	0.60 (0.05) ^{ns}
(10) Tree aboveground CUE [7/(7 + 8)]	0.41 (0.02)	0.48 (0.01)**
(11) Understory photosynthesis	27 (3)	58 (2)*
<i>Belowground</i>		
(12) Tree coarse root production	12 (2)	25 (3)**
(13) Net soil organic carbon production	5 (1.4)	109 (7)
(14) Soil respiration	492 (20)	323 (10)***
(15) Total belowground flux (TBCF) [12 + 13 + 14 – 3 – 4]	417 (25)	297 (17)**
(16) Fine-root, mycorrhiza, and exudate production [15 – 12 – 13]	400 (24)	163 (15)***
<i>Summation</i>		
(17) Photosynthesis (GPPCF) [7 + 8 + 11 + 15]	955 (32)	1104 (29)*
(18) Ecosystem respiration (RecoCF) [1 + 2 + 14]	795 (24)	715 (21)*
(19) Net ecosystem production (NEPCF) [17 – 18]	160 (40)	389 (36)**

Fluxes and derived values (indented) are provided to explain how fluxes were combined. The bracketed [] numerals explain how derived terms were calculated from the numbered lines higher in the table. The parenthetical () values are SDs based on error propagation of annual sums. The blue box contains the unitless efficiencies. The yellow box contains, in bold, the ecosystem-scale summations, which are compared to eddy covariance data in the text. *P*-values of paired *t*-tests are designated as: *, *P* < 0.05; **, *P* < 0.01; ***, *P* < 0.001; ns, not significant. The blue box contains efficiencies, which are unitless, unlike the rest of the measurements in the table, which are expressed in g C m⁻² yr⁻¹. The yellow box contains the stand-scale summations of the component fluxes. ANPP, aboveground net primary production; CUE, carbon-use efficiency.

from 0.47 in the Reference plot to 0.42 g C m⁻³ in the Fertilized plot. Leaf litterfall rates increased gradually after the fertilization, also nearly doubling in 2011, but the treatment differences eventually stabilized at 64 ± 18 g C m⁻² yr⁻¹ (Fig. 2; Table 3). The steady state in litterfall allowed us to use the litterfall rate as an estimate of annual production of transient tissues, including leaves, in the carbon budgets that follow. The steady state described here was attained near the end of the data reported in an earlier description of biomass production on this site (2006–2013; Lim *et al.*, 2015).

Belowground component fluxes

Combined soil and understory respiration rates were 52% higher on the Reference plot than on the Fertilized plot (Table 3). The

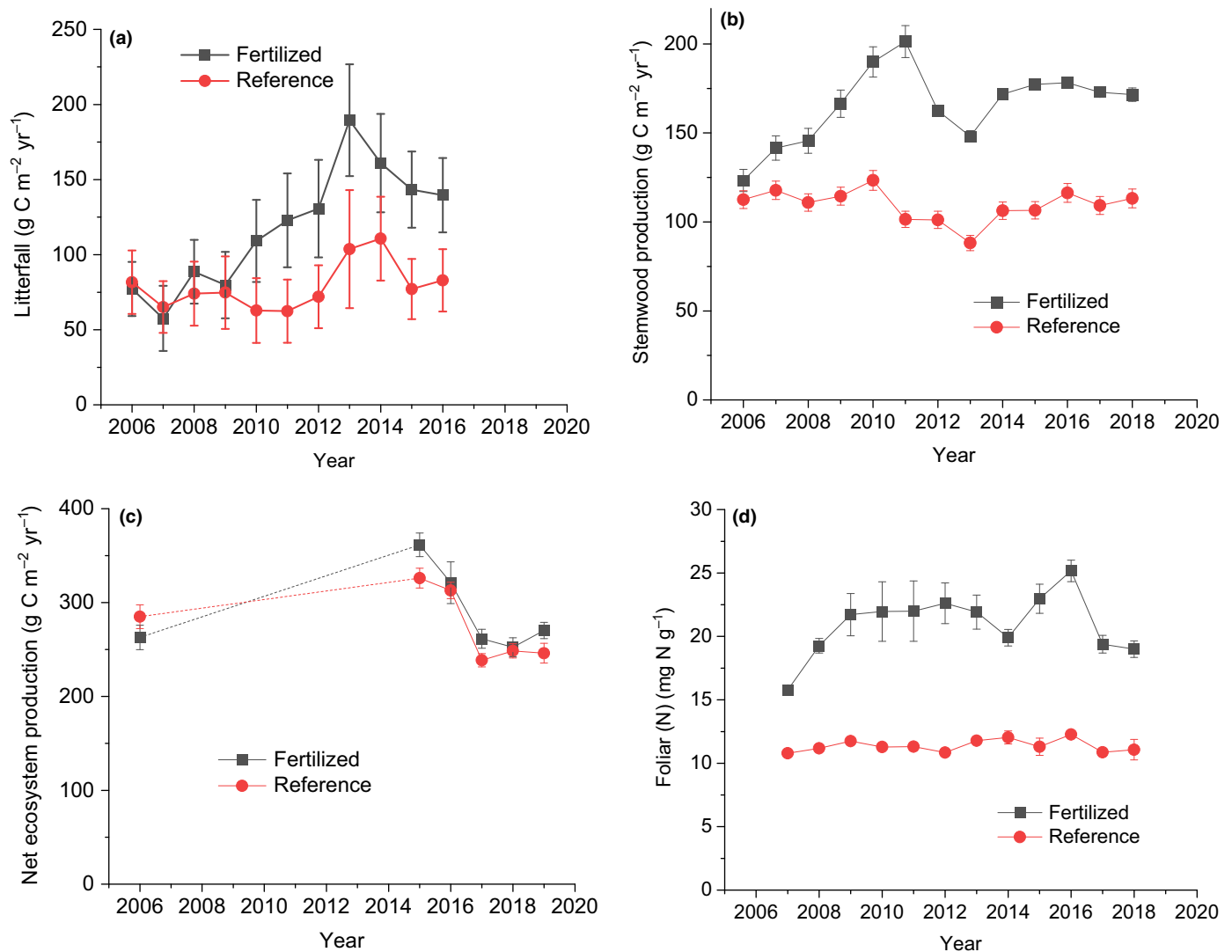


Fig. 2 Time series data showing approach to new steady state after repeated annual nitrogen fertilizations of Scots pine for (a) litterfall, (b) stemwood production, (c) net ecosystem production (NEP) by eddy covariance, and (d) foliar nitrogen concentration with SD error bars. The steady-state assumption allows us to combine component measurements from different years and to use estimates of litterfall to infer production. The dashed line in (c) emphasizes the long extrapolation necessary in the NEP data.

difference nearly disappeared in the wintertime, and it increased sharply soon after the commencement of canopy photosynthesis, driven by increases in base respiration rates. Soil organic matter production was increased sharply by the fertilization, from 5 ± 2 to $109 \pm 7 \text{ g C m}^{-2} \text{ yr}^{-1}$ (Table 3). The total belowground carbon flux, estimated from the sum of these changes, was 29% lower on the Fertilized plot than on the Reference plot (Fig. 3; Table 2). Fine-root, mycorrhiza, and exudate (FRME) production accounted for 400 ± 24 and $163 \pm 15 \text{ g C m}^{-2} \text{ yr}^{-1}$ in the Reference and Fertilized plots, respectively, which is a reduction of 59% on the fertilized plot (Table 3).

GPP and R_{eco} from component fluxes

For the first time at this site, we have assembled all the component fluxes, yielding a total GPP of 990 ± 32 and $1100 \pm$

$29 \text{ g C m}^{-2} \text{ yr}^{-1}$ on the Reference and the Fertilized plot, respectively (Fig. 3; Table 3). Of these totals, 62 and $53 \text{ g C m}^{-2} \text{ yr}^{-1}$ were due to understory GPP, corresponding to only 6 and 5% of total GPP. The component fluxes are presented as raw fluxes in Table 3 and as percentages of component-derived GPP in Fig. 4. Partitioning to all components was increased by fertilization, except fine-root, mycorrhiza, and exudate production, which decreased from 40 ± 2.5 to $15 \pm 1.4\%$ of GPP (Fig. 5). This reduction decreased cumulative belowground partitioning (TBCF) from 42 (2.5%) in the Reference plot to $27 \pm 1.5\%$ in the Fertilized plot. The respiratory components were summed to yield R_{eco} estimates of 795 ± 24 and $715 \pm 21 \text{ g C m}^{-2} \text{ yr}^{-1}$ (Table 3). The NEP estimates from these component fluxes were 160 ± 40 and $389 \pm 36 \text{ g C m}^{-2} \text{ yr}^{-1}$ for the Reference and Fertilized plots, respectively (Table 3).

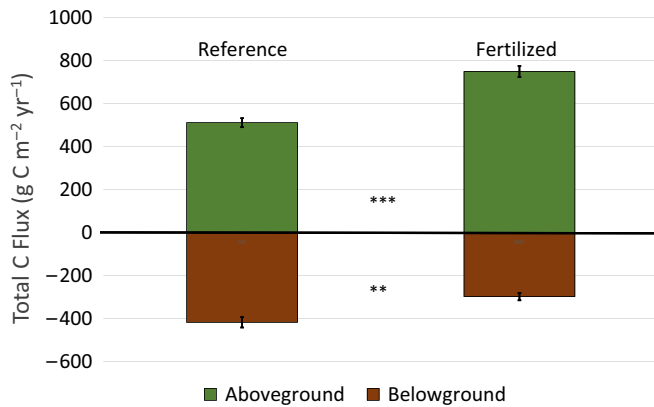


Fig. 3 Aboveground and belowground carbon fluxes from the Reference and Fertilized Scots pine plots at Rosinedal, Sweden, with SD error bars. Asterisks describe the significance levels of *t*-tests based on propagated error: *, *P* < 0.05; **, *P* < 0.01; ***, *P* < 0.001. The belowground fluxes are presented as negative numbers. The aboveground flux is estimated by summing aboveground net primary production (NPP) and aboveground respiration. The belowground flux is total belowground carbon flux (TBCF). The total height of the bar, including both aboveground and belowground components, is gross primary production (GPP). The upward shift in the Fertilized plot reflects the shift toward aboveground partitioning.

Carbon-use efficiency

Annual stem and leaf respiration fluxes were somewhat higher on the Fertilized plot, 111 ± 16 vs 93 ± 10 $\text{g C m}^{-2} \text{yr}^{-1}$ for stems and branches and 281 ± 9 vs 210 ± 8 $\text{g C m}^{-2} \text{yr}^{-1}$ for leaves (Table 3). The resulting aboveground CUE values were 0.41 ± 0.02 $\text{g C biomass}^{-1} \text{C in AGPP}$ for the Reference and 0.48 ± 0.01 $\text{g C NPP g}^{-1} \text{C in AGPP}$ for the Fertilized plot (Fig. 6; Table 3). The CUE of stem and branches alone yielded somewhat higher values: 0.53 ± 0.02 g g^{-1} for the Reference and 0.60 ± 0.05 g g^{-1} for the Fertilized. Belowground CUE was 0.31 and 0.53 $\text{g C biomass}^{-1} \text{C TBCF}$ on the Reference and Fertilized plots, respectively (Fig. 6). Total CUE was 0.37 for the Reference plot and 0.49 for the Fertilized plot.

Eddy covariance estimates of ecosystem fluxes

The EC-based GPP estimates were 935 ± 74 and 1056 ± 68 $\text{g C m}^{-2} \text{yr}^{-1}$ for the Reference and Fertilized plots, respectively (Fig. 7). The treatment difference was significant (at *P* < 0.05). The R_{eco} based on EC averages was 660 ± 38 $\text{g C m}^{-2} \text{yr}^{-1}$ for the Reference

Fig. 4 Component fluxes on the Reference and Fertilized Scots pine plots, expressed as percentages of gross primary production (GPP) (with SD in parentheses). The data are from Table 3. The arrow widths are proportional to the fluxes. GPP of the understory was small and was not divided into components, but it was added into the GPP estimate from the sum of components.

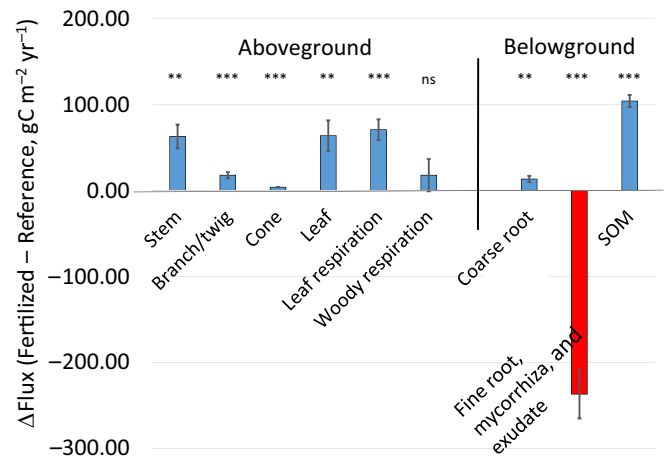
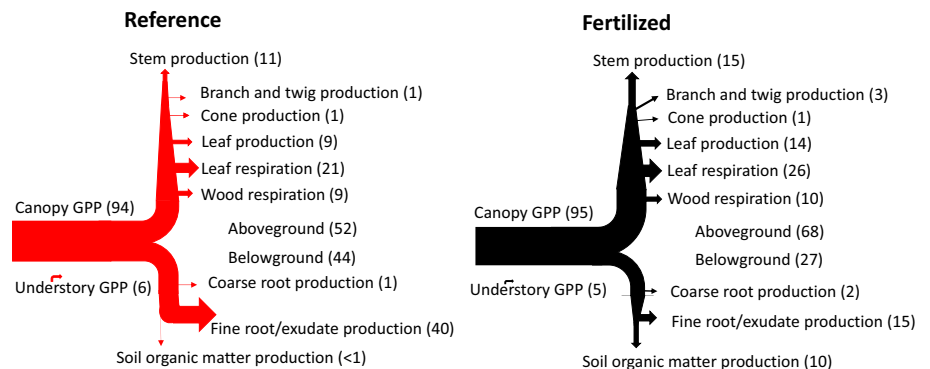


Fig. 5 Fertilizer-induced changes in partitioning (Fertilized – Reference) in Scots pine. Partitioning is expressed relative to gross primary production (GPP), with SD error bars. Fertilizer increases partitioning to all components except fine-root, mycorrhiza, and exudate (FRME) production. Therefore, we can attribute at least part of the increase in stemwood production to the partitioning shift away from fine-root and exudate production. Asterisks describe the significance levels of *t*-tests based on propagated error: *, *P* < 0.05; **, *P* < 0.01; ***, *P* < 0.001. ns, not significant; SOM, soil organic matter.

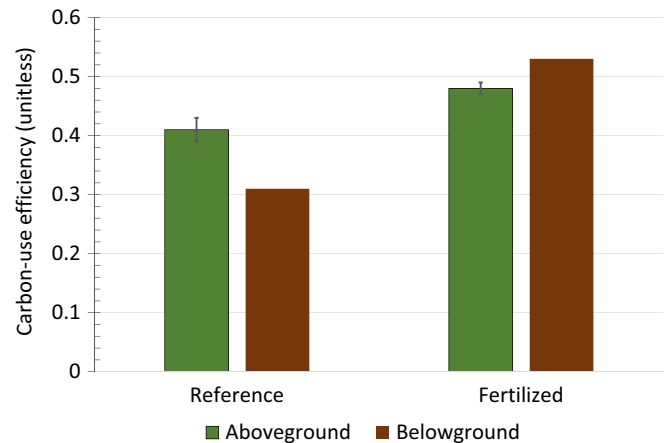


Fig. 6 Carbon-use efficiencies aboveground and belowground on the Reference and Fertilized Scots pine plots, with SD error bars.

and 762 ± 37 $\text{g C m}^{-2} \text{yr}^{-1}$ for the Fertilized plot (Fig. 7). Thus, the fertilization increased R_{eco} ($+102 \pm 53$ $\text{g C m}^{-2} \text{yr}^{-1}$), but had no effect on NEP $+19 \pm 62$ $\text{g C m}^{-2} \text{yr}^{-1}$, according to EC (Fig. 8).

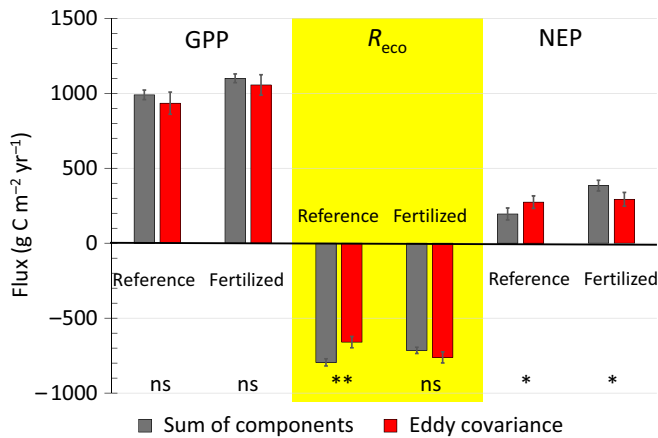


Fig. 7 Comparison of whole-ecosystem fluxes by summed components vs eddy covariance (average of 2015–2019) in Scots pine forest plots, with SD error bars. Asterisks describe the significance levels of *t*-tests based on propagated error: *, $P < 0.05$; **, $P < 0.01$; ***, $P < 0.001$. GPP, gross primary production; NEP, net ecosystem production; ns, not significant; R_{eco} , ecosystem respiration.

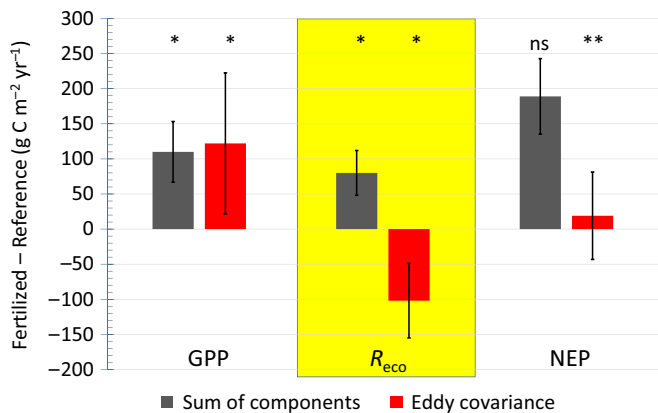


Fig. 8 Comparison of plot differences in ecosystem fluxes as measured by summed components vs eddy covariance in Scots pine forest plots, with SD error bars. Asterisks describe the significance levels of *t*-tests based on propagated error: *, $P < 0.05$; **, $P < 0.01$; ***, $P < 0.001$. GPP, gross primary production; NEP, net ecosystem production; ns, not significant; R_{eco} , ecosystem respiration.

Method comparison

We next compared the nitrogen fertilization responses between the methods. Both methods detected a fertilization-induced increase in GPP, by 121 ± 100 and 110 ± 44 $\text{g C m}^{-2} \text{yr}^{-1}$ for EC and components, respectively (Fig. 8). R_{eco} increased by 102 ± 53 $\text{g C m}^{-2} \text{yr}^{-1}$ according to eddy covariance, but it decreased by 80 ± 32 $\text{g C m}^{-2} \text{yr}^{-1}$ according to the component fluxes (Fig. 8). Although these changes in R_{eco} were in opposite directions, they were both significant (Fig. 8). These differences also appeared in the NEP data, where the sum of components found that the Fertilized plot was significantly higher, by 229 ± 54 $\text{g C m}^{-2} \text{yr}^{-1}$ than the Reference plot (Figs 7, 8), but eddy covariance detected no significant difference ($+19 \pm 62$ $\text{g C m}^{-2} \text{yr}^{-1}$; Figs 7, 8).

Discussion

Before nitrogen fertilization, the fertilized plot began with a carbon budget similar to that of the Reference (Zhao *et al.*, 2022) despite small differences in stand characteristics (Lim *et al.*, 2015). Five years of annual fertilization were required to reach a new steady state in the component fluxes. The new steady state was reflected in the higher litterfall, stemwood production, and foliar nitrogen concentration reported here, as well as the recent report of NEP (Fig. 2; Zhao *et al.*, 2022). These variables continued to fluctuate from year to year, but the differences between the plots became stable and there was no longer an obvious temporal trend. The steady state occurred here because the fertilization recurred annually, maintaining high N status continually. The study differs from operational forest fertilization scenarios, which typically occur in a single year at long intervals rather than being repeated annually (Fisher & Binkley, 2000; Lim *et al.*, 2020). It was useful here because it allowed us to combine component flux estimates made in different years and to use compartmental losses, for example, litterfall (Fig. 2a), as estimates of compartmental gains, for example, leaf production. It also provided an extreme example of the influence of nitrogen fertilization in such forests.

The fertilization caused significant changes in all stand-level component fluxes except stem respiration. The largest flux increases were in SOC formation (104 ± 7 (SD) $\text{g C m}^{-2} \text{yr}^{-1}$), leaf respiration (71 ± 12 $\text{g C m}^{-2} \text{yr}^{-1}$), leaf production (64 ± 18 $\text{g C m}^{-2} \text{yr}^{-1}$), and stem production (63 ± 14 $\text{g C m}^{-2} \text{yr}^{-1}$). All component flux changes were positive except fine-root, mycorrhizae, and exudate (FRME) production, which decreased sharply (Fig. 5). We therefore conclude that the reduction in partitioning to FRME production was a major source of the photosynthate used for the increases in the other fluxes. This conclusion depends on the assumption that the system was at steady state, for example, in canopy biomass. If so, we could use litterfall to estimate leaf production. Although litterfall varies from year to year, the mean rates were calculated over 6 yr after 2012, during which the upward trend on the fertilized plot had ceased. This approach yields average partitioning values over the period. Although annual changes in partitioning would be interesting, we considered them beyond the scope of the current study.

Aboveground carbon-use efficiency estimated from aboveground fluxes increased from 0.41 ± 0.02 – 0.48 ± 0.01 by fertilization (Table 3). These estimates are rigorous because they are almost uninfluenced by heterotrophic respiration. In addition, the respiration rates used to calculate them had low standard errors and were measured over most of the growing season. The primary controls over ACUE are the amount of maintenance respiration and the chemical composition of the tissue produced. Although the growth respiration estimate is well constrained by the most efficient pathways of biosynthesis (Vertregt & Penning de Vries, 1987), the amount of maintenance respiration is theoretically unconstrained. In practice, maintenance respiration seems to vary rather little (e.g. Ryan & Waring, 1992). The ACUE of stems and branches was somewhat higher: 0.53 and 0.60 for the Reference and Fertilized plots, respectively. We speculate that this higher CUE was caused at least in part by stem photosynthesis, which is relatively high

under the smooth bark of the upper stems and branches of Scots pine (Tarvainen *et al.*, 2021). Stem photosynthesis uses part of the radial diffusion of CO₂ generated in biosynthetic processes and increases ACUE by reducing the net outward CO₂ efflux. Partitioning shifts have no influence on ACUE because it is based exclusively on aboveground measurements.

There has been some controversy about the constancy of ecosystem-scale CUE (Waring *et al.*, 1998; Mäkelä & Valentine, 2001; Collalti & Prentice, 2019; Landsberg *et al.*, 2020). Our aboveground estimates are significantly different ($P < 0.01$; Table 3). However, BCUE is more difficult to assess. The difficulty begins with the definitions of heterotrophic and autotrophic fluxes, which may or may not include mycorrhizal fungi, other rhizosphere organisms, and autotrophic priming of heterotrophic respiration (Högberg & Read, 2006; Marshall *et al.*, 2021). The root respiration term must be added to inferred R_a because roots continue to respire in the wintertime (Schindlbacher *et al.*, 2007), which would be misattributed to heterotrophic respiration rather than R_a by the Pumpanen *et al.* (2015) method that we used.

We speculate that the observed difference in BCUE was caused by the priming of heterotrophic respiration, which increased the respiration rate without measurable increases in biomass. Priming was considered to have been shut off by the fertilization (Bonner *et al.*, 2019; Marshall *et al.*, 2021). Alternatively, fertilization may have reduced the 'wasteful' alternative oxidase (AOX) pathway in favor of the efficient cytochrome oxidase (COX) pathway (Henriksen *et al.*, 2019). Previous data from this site found that the AOX pathway accounted for 23% (± 0.2) of root respiration in the Reference stand, but only 14% (± 0.2) in the Fertilized stand (Henriksen *et al.*, 2019). The increase in BCUE on the fertilized plot agrees with (Capioli *et al.*, 2015), who used a different terminology to describe similar phenomena in managed vs unmanaged forests.

Most previous estimates of partitioning have relied on BNPP. BNPP may be defined to include mycorrhizal respiration, oxidation of exudates and priming of heterotrophic substrates. In addition, the uncertainty of turnover rates for hyphal and other rhizosphere biomass makes it difficult to determine an NPP value (Capioli *et al.*, 2016; Marshall *et al.*, 2021). For these reasons, we argue that the TBCF parameter is a more quantitatively rigorous measure of belowground carbon partitioning. A recent study using TBCF in a temperate hardwood forest (Eastman *et al.*, 2021) found that fertilization decreased TBCF by 114 g C m⁻² yr⁻¹, almost the same as the 124 g C m⁻² yr⁻¹ reduction observed here (Table 3).

We next quantified the causes of the fertilizer-induced increase in stemwood growth (Table 4). The stemwood increase was a surprisingly small proportion of the carbon budget, increasing the proportion of GPP from only 11 to 15%. The actual increase was 63 \pm 14 g C m⁻² yr⁻¹. Such a small amount of carbon could theoretically have come from a decrease in any of several other components. However, the only decrease in partitioning observed here was in FRME production (Figs 4, 5), which decreased from 400 \pm 24 to 163 \pm 15 g C m⁻² yr⁻¹ (Table 3). This decrease is easily sufficient to supply the carbon required for the stemwood growth increase.

Because the changes in GPP, CUE, and partitioning are multiplicative, we began by estimating the change in stemwood

Table 4 Description of causes of fertilizer-induced Scots pine stemwood growth increase based on component fluxes in Table 3.

Source	g C m ⁻² yr ⁻¹	%
(20) Δ stemwood production (F5 – R5)	63	100
(21) GPP effect (F17/R17) \times R5 – R5	17	26
(22) CUE effect (F9 – R9) \times (R5 + R21)	9	14
(23) Partitioning effect (20 – 21 – 22)	38	60

Parenthetical calculations refer to fluxes presented in Table 3, where R refers to Reference, F to Fertilized, and the numerals to the numbered lines.

production due to the GPP increase as if partitioning and CUE were constant (Table 4). By itself, this GPP effect would increase stem production by 17 g C m⁻² yr⁻¹. Because the CUE of stem and branch production also increased, we estimated that effect as well. Here, we have multiplied the GPP-corrected stem and branch production by the increase in CUE, yielding 9 g C m⁻² yr⁻¹. We attribute the remainder to a shift in partitioning. We can thus ascribe 26% (17/63) of the increase in stem growth to increased GPP, 14% (9/63) to increased CUE, and the remaining 60% to reallocation away from fine root, mycorrhiza, and exudate production (Table 4). Given the long-term, heavy fertilization applied here, these nitrogen responses probably approach the maximum possible in mature boreal Scots pine.

Our second objective was to compare the eddy covariance data to the component fluxes. A decoupling filter was applied to eliminate periods when the air mass below the canopy was isolated from that above, and flowing as advection into the river valley adjacent to the research plots (Jocher *et al.*, 2017, 2018). The decoupling filter reduced the annual net CO₂ uptake by 22% relative to the traditional u^* filtering approach (Jocher *et al.*, 2018). Similar comparisons of component fluxes to eddy covariance have been carried out elsewhere (Zha *et al.*, 2007; Capioli *et al.*, 2016). However, we are not aware of a previous instance where decoupling-corrected EC data have been used in such a comparison or where the components have been measured so rigorously.

The EC estimates of GPP were 55 \pm 81 and 44 \pm 74 g C m⁻² yr⁻¹ lower than the GPP estimates from sum of components for the Reference and Fertilized plots, respectively, but the differences were not significant (Fig. 7). This agreement occurred despite the complete independence of these methods. A third estimate of GPP at Rosinedal was based on a model of these plots (Tian *et al.*, 2021). Those estimates (914 and 1132 g C m⁻² yr⁻¹ for Reference and Fertilization, respectively) also agree rather well with ours, although they were not entirely independent as the model was parameterized with site-specific EC data. Another comparison, which relies on independent methods combining sap flux with water-use efficiency from stable isotope composition, was recently published (Vernay *et al.*, 2020). The daily values in the summer agree well with the estimates here, but the isotopic estimates were higher in the fall. On the compartmental flux side, initial comparisons of the photosynthetic rates using branch cuvettes found no differences in long-term photosynthetic performance per unit leaf area between the plots (Tarvainen *et al.*, 2016). This was attributed in part to the storage of nitrogen in forms that did not contribute to

photosynthetic rates, primarily free amino acids. The observed increase in GPP, but not leaf-scale photosynthesis, could still occur if the differences in GPP were due to higher leaf area index on the fertilized plot (Table 2), particularly during the summer maximum of LAI (Lim *et al.*, 2015).

R_{eco} on the Reference plot was 135 ± 45 higher in the EC data than in the component fluxes. In contrast, the method difference on the Fertilized plot was not significant. The chamber data were based on continuous measurements throughout the growing season, so it is unlikely that the difference is due to a seasonal sampling bias. The shoot respiration fluxes were measured from closed cuvettes placed on 1-year-old shoots. The stem respiration fluxes were likewise measured from closed cuvettes. They were placed on the lower stem where bark photosynthesis was minimal. However, we separately measured the magnitude of bark photosynthesis, which reduces bark efflux, on the upper stems and accounted for it in the upscaling (Tarvainen *et al.*, 2018). Similarly, daytime reductions in respiration rate have often been neglected in this kind of study (Capioli *et al.*, 2016; Wehr *et al.*, 2016). However, we made this correction. There have been worries that xylem water fluxes might carry dissolved CO_2 away from the sites of respiration toward the canopy, which could bias estimates of stem, root, and soil respiration. However, we demonstrated using a labeled tracer that such fluxes were minimal at our site, perhaps due to the low pH and hence low solubility of CO_2 in xylem sap of pines (Tarvainen *et al.*, 2021, 2023).

We sampled forest-floor respiration over the whole contents of large-footprint chambers ($< 20 \text{ m}^2$) every 30 min for most of three growing seasons. Several issues relating to these chambers were addressed in an earlier paper (Marshall *et al.*, 2021). The soil respiration rates estimated by the control chambers were similar to those estimated for soil + understory by below-canopy EC measurements in the control stand (Chi *et al.*, 2021). The reasonability of the CUE estimates derived from them further argues for their validity. However, despite their large size, the chambers sampled a much smaller area than the EC footprint (40 m^2 vs $160\,000 \text{ m}^2$).

Method differences in NEP were significant for both methods, but in opposite directions between the plots. The EC-based NEP was $79 \pm 58 \text{ g C m}^{-2} \text{ yr}^{-1}$ higher on the Reference plot vs $91 \pm 58 \text{ g C m}^{-2} \text{ yr}^{-1}$ lower on the Fertilized plot. Although we cannot explain this behavior, it is cause for concern. These issues are reminiscent of an earlier study that found disagreement between chamber methods and eddy covariance in montane spruce-fir forest under bark-beetle attack (Speckman *et al.*, 2015). In that study, bark beetles killed or impaired 85% of the basal area, yet EC detected no change in R_{eco} , while chamber measurements did. The authors speculated that the loss of foliage from the dead trees improved the coupling of the ground to the atmosphere, compensating for true reductions in R_{eco} after the mortality. That cannot explain the discrepancies in the current study because (1) canopy LAI was not greatly different between the plots and (2) we corrected our EC data for decoupling.

Capioli *et al.* (2016) raised several important questions about bottom-up vs top-down comparisons such as this one. First, they noted that the component flux method is in fact an

unstandardized mixture of different methods and approaches. Here, we have tried to use the most rigorous and up-to-date methods available to deliver measurements that are both accurate and precise. The design and performance of the soil chambers are especially noteworthy, as are the continuous measurements of leaf and stem gas exchange and the careful estimation of TBCF. Second, they noted that boreal forests tended to be especially problematic in these comparisons, presumably because their fluxes were small. We speculate that canopy decoupling, which is not routinely accounted for in EC studies, may explain part of this discrepancy. Third, Capioli *et al.* (2016) pointed out that nonsteady-state through-flow chambers (NSF), which we have used here, yield higher respiration fluxes than from EC methods. However, as noted earlier, our chambers agreed well with below-canopy EC estimates (Chi *et al.*, 2021).

As observed elsewhere (e.g. Olsson *et al.*, 2005; Maaroufi *et al.*, 2015; Forsmark *et al.*, 2020), the soil was accumulating organic matter rapidly under the high fertilization. This accumulation was included by definition in the component flux summation (item 13 in Table 3), but was not reflected in the R_{ecoEC} estimates from eddy flux. The increases in SOC accumulation (Marshall *et al.*, 2021; $104 \text{ g C m}^{-2} \text{ yr}^{-1}$) and stemwood production ($63 \text{ g C m}^{-2} \text{ yr}^{-1}$) together represent 74% (169/229) of the increase in NEP, according to component fluxes, following fertilization. However, these carbon accumulations represent nine times (169/19) the increase in NEP according to eddy covariance. It is difficult to understand how the eddy covariance estimate did not detect the increase in SOC and biomass production. Conceivably, these increases in NEP were offset by decreases in some other C sink, but it is not clear what that would be. There was a strong reduction in the flux to FRME, but these pools turn over so rapidly that they would not constitute a long-term sink.

Apart from our own study (Zhao *et al.*, 2022), few have applied eddy covariance to study the influence of N fertilization on carbon fluxes. In one, young Douglas-fir forests were compared for 5 yr before and after a single fertilization event (Lee *et al.*, 2020). Nitrogen effects on GPP were minor, but R_{eco} was sharply reduced and NEP increased. Another (El-Madany *et al.*, 2021) examined fertilization effects on a Mediterranean savannah. The fertilization shifted the system from a net C source to neutral. In our previous study, where we estimated errors differently, we also concluded that NEP was significantly increased by the N fertilization. In summary, all these studies have found increased NEP due to fertilization, as we did with component fluxes, but not with EC.

Conclusions

We have provided a detailed ecophysiological description of changes in C sources, sinks, and fluxes when a boreal forest is heavily and continuously nitrogen-fertilized. The accumulations in SOC and biomass and the flux to fine roots, mycorrhizae, and exudates were of particular importance. When summed into an estimate of NEP, these changes yield a nitrogen-induced increase. However, eddy covariance did not detect this increase. The measurements were not made in the same years, which is suboptimal.

However, as the systems have been considered at steady state (Zhao *et al.*, 2022), we argue that the temporal mismatch should not matter, at least not when comparing means over several years. We call for similar experiments, addressing the influence of nitrogen fertilization in simple ecosystems, where the two methods can be compared.

Acknowledgements

The Rosinedalsheden research site was established with support from the Kempe Foundation and the Swedish Research Council for Environment, Agricultural Sciences and Spatial Planning (FORMAS) and has since 2014 been part of the 'Swedish Infrastructure for Ecosystem Science' (SITES) sponsored by the Swedish Science Foundation (VR). This study received support from the Swedish Governmental Agency for Innovation Systems (VINNOVA), FORMAS and The Strategic Research Area 'Biodiversity and Ecosystem Services in a Changing Climate' (BECC). We thank Jan Parsby for designing the soil chambers and, together with Thomas Hörnlund and Giuseppe DeSimon, for installation and maintenance of chambers and sensors. JDM and MP were supported in part by the Knut and Alice Wallenberg Foundation (nos. 2015.0047 and 2018.0259). We want to commemorate our colleague and dear friend Mats Råntfors, who has been vital in the setup of the experiment and the maintenance of the gas-exchange system.










Competing interests

None declared.

Author contributions

JDM, GW, SL and MP contributed to conceptualization, methodology, and writing. LT contributed to methodology, investigation, and writing. PZ contributed to investigation and writing. HL contributed to investigation. TN and TL contributed to conceptualization and administration.

ORCID

Hyungwoo Lim  <https://orcid.org/0000-0001-9457-7203>
 Sune Linder  <https://orcid.org/0000-0001-9036-5422>
 Tomas Lundmark  <https://orcid.org/0000-0003-2271-3469>
 John D. Marshall  <https://orcid.org/0000-0002-3841-8942>
 Torgny Näsholm  <https://orcid.org/0000-0002-2275-2030>
 Matthias Pechl  <https://orcid.org/0000-0002-9940-5846>
 Lasse Tarvainen  <https://orcid.org/0000-0003-3032-9440>
 Göran Wallin  <https://orcid.org/0000-0002-5359-1102>
 Peng Zhao  <https://orcid.org/0000-0003-3289-5067>

Data availability

The data that support the findings of this study are available from the Swedish National Data Repository at <https://doi.org/10.5878/3yfv-pg60>.

References

- Axelsson E, Axelsson B. 1986. Changes in carbon allocation patterns in spruce and pine trees following irrigation and fertilization. *Tree Physiology* 2: 189–204.
- Baldocchi D. 2008. 'Breathing' of the terrestrial biosphere: lessons learned from a global network of carbon dioxide flux measurement systems. *Australian Journal of Botany* 56: 1–26.
- Bonner MTL, Castro D, Schneider AN, Sundström G, Hurry V, Street NR, Näsholm T. 2019. Why does nitrogen addition to forest soils inhibit decomposition? *Soil Biology and Biochemistry* 137: 107570.
- Campioi M, Malhi Y, Vicca S, Luysaert S, Papale D, Peñuelas J, Reichstein M, Migliavacca M, Arain MA, Janssens IA. 2016. Evaluating the convergence between eddy-covariance and biometric methods for assessing carbon budgets of forests. *Nature Communications* 7: 13717.
- Campioi M, Vicca S, Luysaert S, Bilcke J, Ceschia E, Chapin Iii FS, Ciais P, Fernández-Martínez M, Malhi Y, Obersteiner M *et al.* 2015. Biomass production efficiency controlled by management in temperate and boreal ecosystems. *Nature Geoscience* 8: 843–846.
- Chi J, Zhao P, Klosterhalfen A, Jocher G, Kljun N, Nilsson MB, Pechl M. 2021. Forest floor fluxes drive differences in the carbon balance of contrasting boreal forest stands. *Agricultural and Forest Meteorology* 306: 108454.
- Collalti A, Prentice IC. 2019. Is NPP proportional to GPP? Waring's hypothesis 20 years on. *Tree Physiology* 39: 1473–1483.
- Duursma RA, Medlyn BE. 2012. MAESPA: a model to study interactions between water limitation, environmental drivers and vegetation function at tree and stand levels, with an example application to [CO₂] × drought interactions. *Geoscientific Model Development* 5: 919–940.
- Eastman BA, Adams MB, Brzostek ER, Burnham MB, Carrara JE, Kelly C, McNeil BE, Walter CA, Peterjohn WT. 2021. Altered plant carbon partitioning enhanced forest ecosystem carbon storage after 25 years of nitrogen additions. *New Phytologist* 230: 1435–1448.
- El-Madany TS, Reichstein M, Carrara A, Martín MP, Moreno G, Gonzalez-Cascon R, Peñuelas J, Ellsworth DS, Burchard-Levine V, Hammer TW *et al.* 2021. How nitrogen and phosphorus availability change water use efficiency in a Mediterranean savanna ecosystem. *Journal of Geophysical Research Biogeosciences* 126: e2020JG006005.
- Fisher RF, Binkley D. 2000. *Ecology and management of forest soils*. New York, NY, USA: John Wiley & Sons.
- Forsmark B, Nordin A, Maaroufi NI, Lundmark T, Gundale MJ. 2020. Low and high nitrogen deposition rates in northern coniferous forests have different impacts on aboveground litter production, soil respiration, and soil carbon stocks. *Ecosystems* 23: 1423–1436.
- Giardina CP, Ryan MG. 2002. Total belowground carbon allocation in a fast-growing Eucalyptus plantation estimated using a carbon balance approach. *Ecosystems* 5: 487–499.
- Goulden ML, Mcmillan AMS, Winston GC, Rocha AV, Manies KL, Harden JW, Bond-Lamberty BP. 2011. Patterns of NPP, GPP, respiration, and NEP during boreal forest succession. *Global Change Biology* 17: 855–871.
- Halbritter A, De Boeck H, Eycott A, Robinson D, Vicca S, Berauer B, Christiansen C, Estiarte M, Grünzweig JM, Gya R *et al.* 2020. The handbook for standardised field measurements in terrestrial global change experiments. *Methods in Ecology and Evolution* 11: 22–37.
- Hasselquist N, Metcalfe DB, Höglberg P. 2012. Contrasting effects of low and high nitrogen additions on soil CO₂ flux components and ectomycorrhizal fungal sporocarp production in a boreal forest. *Global Change Biology* 18: 3596–3605.
- Henriksson N, Marshall J, Lundholm J, Boily Å, Boily J-F, Näsholm T. 2019. Improved *in vivo* measurement of alternative oxidase respiration in field-collected pine roots. *Physiologia Plantarum* 167: 34–47.
- Höglberg P, Read DJ. 2006. Towards a more plant physiological perspective on soil ecology. *Trends in Ecology & Evolution* 21: 548–554.
- Janssens IA, Dieleman W, Luysaert S, Subke J-A, Reichstein M, Ceulemans R, Ciais P, Dolman AJ, Grace J, Matteucci G *et al.* 2010. Reduction of forest soil respiration in response to nitrogen deposition. *Nature Geoscience* 3: 315–322.

- Jocher G, Marshall J, Nilsson MB, Linder S, De Simon G, Hörnlund T, Lundmark T, Näsholm T, Ottosson Löfvenius M, Tarvainen L *et al.* 2018. Impact of canopy decoupling and subcanopy advection on the annual carbon balance of a boreal Scots pine forest as derived from eddy covariance. *Journal of Geophysical Research: Biogeosciences* 123: 303–325.
- Jocher G, Ottosson Löfvenius M, De Simon G, Hörnlund T, Linder S, Lundmark T, Marshall J, Nilsson MB, Näsholm T, Tarvainen L *et al.* 2017. Apparent winter CO₂ uptake by a boreal forest due to decoupling. *Agricultural and Forest Meteorology* 232: 23–34.
- Landsberg JJ, Waring RH, Williams M. 2020. The assessment of NPP/GPP ratio. *Tree Physiology* 40: 695–699.
- Laudon H, Taberman I, Ågren A, Futter M, Ottosson-Löfvenius M, Bishop K. 2013. The Krycklan Catchment Study – a flagship infrastructure for hydrology, biogeochemistry, and climate research in the boreal landscape. *Water Resources Research* 49: 7154–7158.
- Lee S-C, Black TA, Jassal RS, Christen A, Meyer G, Nesic Z. 2020. Long-term impact of nitrogen fertilization on carbon and water fluxes in a Douglas-fir stand in the Pacific Northwest. *Forest Ecology and Management* 455: 117645.
- Lim H, Olsson BA, Lundmark T, Dahl J, Nordin A. 2020. Effects of whole-tree harvesting at thinning and subsequent compensatory nutrient additions on carbon sequestration and soil acidification in a boreal forest. *GCB Bioenergy* 12: 992–1001.
- Lim H, Oren R, Palmroth S, Tor-ngern P, Mörling T, Näsholm T, Lundmark T, Helmisaari H-S, Leppälampi-Kujansuu J, Linder S. 2015. Inter-annual variability of precipitation constrains the production response of boreal *Pinus sylvestris* to nitrogen fertilization. *Forest Ecology and Management* 348: 31–45.
- Linder S, Axelsson B. 1982. Changes in carbon uptake and allocation patterns as a result of irrigation and fertilization in a young *Pinus sylvestris* stand. In: Waring RH, ed. *Carbon uptake and allocation in subalpine ecosystems as a key to management*. Corvallis, OR, USA: Oregon State University, 38–44.
- Litton CM, Raich JW, Ryan MG. 2007. Carbon allocation in forest ecosystems. *Global Change Biology* 13: 2089–2109.
- Maaroufi NI, Nordin A, Hasselquist NJ, Bach LH, Palmqvist K, Gundale MJ. 2015. Anthropogenic nitrogen deposition enhances carbon sequestration in boreal soils. *Global Change Biology* 21: 3169–3180.
- Mäkelä A, Valentine HT. 2001. The ratio of NPP to GPP: evidence of change over the course of stand development. *Tree Physiology* 21: 1015–1030.
- Manzoni S, Čapek P, Porada P, Thurner M, Winterdahl M, Beer C, Brüchert V, Frouz J, Herrmann AM, Lindahl BD *et al.* 2018. Reviews and syntheses: carbon use efficiency from organisms to ecosystems – definitions, theories, and empirical evidence. *Biogeosciences* 15: 5929–5949.
- Marshall JD, Peichl M, Tarvainen L, Lim H, Lundmark T, Näsholm T, Öquist M, Linder S. 2021. A carbon-budget approach shows that reduced decomposition causes the nitrogen-induced increase in soil carbon in a boreal forest. *Forest Ecology and Management* 502: 119750.
- Medlyn BE. 1998. Physiological basis of the light use efficiency model. *Tree Physiology* 18: 167–176.
- Monson R, Baldocchi D. 2014. *Terrestrial biosphere-atmosphere fluxes*. Cambridge, UK: Cambridge University Press.
- Olsson P, Linder S, Giesler R, Högberg P. 2005. Fertilization of boreal forest reduces both autotrophic and heterotrophic soil respiration. *Global Change Biology* 11: 1745–1753.
- Peichl M, Brodeur JJ, Khomik M, Arain MA. 2010. Biometric and eddy-covariance based estimates of carbon fluxes in an age-sequence of temperate pine forests. *Agricultural and Forest Meteorology* 150: 952–965.
- Peltoniemi M, Mäkipää R, Liski J, Tamminen P. 2004. Changes in soil carbon with stand age – an evaluation of a modelling method with empirical data. *Global Change Biology* 10: 2078–2091.
- Pumpanen J, Kulmala L, Lindén A, Kolari P, Nikinmaa E, Hari P. 2015. Seasonal dynamics of autotrophic respiration in boreal forest soil estimated by continuous chamber measurements. *Boreal Environment Research* 20: 637–650.
- Raich JW, Nadelhoffer KJ. 1989. Belowground carbon allocation in forest ecosystems: Global trends. *Ecology* 70: 1346–1354.
- Reichstein M, Falge E, Baldocchi D, Papale D, Aubinet M, Berbigier P, Bernhofer C, Buchmann N, Gilmanov T, Granier A *et al.* 2005. On the separation of net ecosystem exchange into assimilation and ecosystem respiration: review and improved algorithm. *Global Change Biology* 11: 1424–1439.
- Ryan MG, Binkley D, Fownes JH, Giardina CP, Senock RS. 2004. An experimental test of the causes of forest growth decline with stand age. *Ecological Monographs* 74: 393–414.
- Ryan MG, Waring RH. 1992. Maintenance respiration and stand development in a subalpine lodgepole pine forest. *Ecology* 73: 2100–2108.
- Schindlbacher A, Zechmeister-Boltenstern S, Glatzel G, Jandl R. 2007. Winter soil respiration from an Austrian mountain forest. *Agricultural and Forest Meteorology* 146: 205–215.
- Speckman HN, Frank JM, Bradford JB, Miles BL, Massman WJ, Parton WJ, Ryan MG. 2015. Forest ecosystem respiration estimated from eddy covariance and chamber measurements under high turbulence and substantial tree mortality from bark beetles. *Global Change Biology* 21: 708–721.
- Stangl ZR, Tarvainen L, Wallin G, Marshall JD. 2022. Limits to photosynthesis: seasonal shifts in supply and demand for CO₂ in Scots pine. *New Phytologist* 233: 1108–1120.
- Tarvainen L, Henriksson N, Näsholm T, Marshall JD. 2023. Among-species variation in sap pH affects the xylem CO₂ transport potential in trees. *New Phytologist* 238: 926–931.
- Tarvainen L, Lutz M, Rantfors M, Näsholm T, Wallin G. 2016. Increased needle nitrogen contents did not improve shoot photosynthetic performance of a mature nitrogen-poor Scots pine trees. *Frontiers in Plant Science* 7: 1051.
- Tarvainen L, Wallin G, Lim H, Linder S, Oren R, Ottosson Löfvenius M, Rantfors M, Tor-Ngern P, Marshall J. 2018. Photosynthetic refixation varies along the stem and reduces CO₂ efflux in mature boreal *Pinus sylvestris* trees. *Tree Physiology* 38: 558–569.
- Tarvainen L, Wallin G, Linder S, Näsholm T, Oren R, Ottosson Löfvenius M, Rantfors M, Tor-Ngern P, Marshall JD. 2021. Limited vertical CO₂ transport in stems of mature boreal *Pinus sylvestris* trees. *Tree Physiology* 41: 63–75.
- Tian X, Minunno F, Schiestl-Aalto P, Chi J, Zhao P, Peichl M, Marshall J, Näsholm T, Lim H, Peltoniemi M *et al.* 2021. Disaggregating the effects of nitrogen addition on gross primary production in a boreal Scots pine forest. *Agricultural and Forest Meteorology* 301–302: 108337.
- Vernay A, Tian X, Chi J, Linder S, Mäkelä A, Oren R, Peichl M, Stangl ZR, Tor-Ngern P, Marshall JD. 2020. Estimating canopy gross primary production by combining phloem stable isotopes with canopy and mesophyll conductances. *Plant, Cell & Environment* 43: 2124–2142.
- Vertregt N, Penning de Vries FWT. 1987. A rapid method for determining the efficiency of biosynthesis of plant biomass. *Journal of Theoretical Biology* 128: 109–119.
- Vicca S, Luysaert S, Peñuelas J, Campioli M, Chapin FS III, Ciais P, Heinemeyer A, Högberg P, Kutsch WL, Law BE *et al.* 2012. Fertile forests produce biomass more efficiently. *Ecology Letters* 15: 520–526.
- Wang YP, Jarvis PG. 1990. Description and validation of an array model – MAESTRO. *Agricultural and Forest Meteorology* 51: 257–280.
- Waring RH, Landsberg JJ, Williams M. 1998. Net primary production of forests: a constant fraction of gross primary production? *Tree Physiology* 18: 129–134.
- Way DA, Yamori W. 2014. Thermal acclimation of photosynthesis: on the importance of adjusting our definitions and accounting for thermal acclimation of respiration. *Photosynthesis Research* 119: 89–100.
- Wehr R, Munger JW, McManus JB, Nelson DD, Zahniser MS, Davidson EA, Wofsy SC, Saleska SR. 2016. Seasonality of temperate forest photosynthesis and daytime respiration. *Nature* 534: 680–683.
- Widén B, Majdi H. 2011. Soil CO₂ efflux and root respiration at three sites in a mixed pine and spruce forest: seasonal and diurnal variation. *Canadian Journal of Forest Research* 31: 786–796.
- Zha T, Xing Z, Wang K-Y, Kellomäki S, Barr AG. 2007. Total and component carbon fluxes of a Scots pine ecosystem from chamber measurements and eddy covariance. *Annals of Botany* 99: 345–353.
- Zhao P, Chi J, Nilsson MB, Ottosson Löfvenius M, Högberg P, Jocher G, Lim H, Mäkelä A, Marshall J, Ratcliffe J *et al.* 2022. Long-term nitrogen addition raises the annual carbon sink of a boreal forest to a new steady-state. *Agricultural and Forest Meteorology* 324: 109112.

Supporting Information

Additional Supporting Information may be found online in the Supporting Information section at the end of the article.

Fig. S1 Component fluxes for the Reference and Fertilized plots expressed in $\text{g C m}^{-2} \text{ yr}^{-1}$, where arrow widths are proportional to the fluxes and SD is shown in parentheses.

Methods S1 Test of age effect on leaf respiration.

Methods S2 Accounting for mortality in stem production estimates.

Methods S3 Error propagation and method comparisons.

Please note: Wiley is not responsible for the content or functionality of any Supporting Information supplied by the authors. Any queries (other than missing material) should be directed to the *New Phytologist* Central Office.

See also the Commentary on this article by Ryan, 239: 2060–2063.